



# Synthesis and structural characterization of zirconium complexes supported by tridentate pyrrolide-imino ligands with pendant N-, O- and S-donor groups and their application in ethylene polymerization

A. C. Pinheiro, S. M. da Silva, Thierry Roisnel, Evgeni Kirillov, Jean-François Carpentier, Osvaldo L. Casagrande

## ► To cite this version:

A. C. Pinheiro, S. M. da Silva, Thierry Roisnel, Evgeni Kirillov, Jean-François Carpentier, et al.. Synthesis and structural characterization of zirconium complexes supported by tridentate pyrrolide-imino ligands with pendant N-, O- and S-donor groups and their application in ethylene polymerization. New Journal of Chemistry, 2018, 42 (2), pp.1477-1483. 10.1039/c7nj04074a . hal-01709533

**HAL Id: hal-01709533**

**<https://univ-rennes.hal.science/hal-01709533>**

Submitted on 26 Apr 2018

**HAL** is a multi-disciplinary open access archive for the deposit and dissemination of scientific research documents, whether they are published or not. The documents may come from teaching and research institutions in France or abroad, or from public or private research centers.

L'archive ouverte pluridisciplinaire **HAL**, est destinée au dépôt et à la diffusion de documents scientifiques de niveau recherche, publiés ou non, émanant des établissements d'enseignement et de recherche français ou étrangers, des laboratoires publics ou privés.

# Synthesis and Structural Characterization of Zirconium Complexes Supported by Tridentate Pyrrolide-Imino Ligands with Pendant *N*-, *O*- and *S*-donor Groups and Their Application in Ethylene Polymerization

A. C. Pinheiro,<sup>a</sup> S. M. da Silva,<sup>a</sup> T. Roisnel,<sup>b</sup> E. Kirillov,<sup>c</sup> J.-F. Carpentier,<sup>c,\*</sup> Osvaldo L. Casagrande Jr.<sup>a,\*</sup>

Zirconium complexes  $\{L\}ZrCl_2(THF)_n$  [ $L = 2-(C_4H_3N-2'-CH=N)C_2H_4NPh$ ,  $x = 3$ ,  $n = 1$ , **2a**;  $L = 2-(C_4H_3N-2'-CH=N)C_6H_4-2-OPh$ ,  $x = 3$ ,  $n = 0$ , **2b**;  $L = 2-(C_4H_3N-2'-CH=N)C_6H_4-2-SPh$ ,  $x = 3$ ,  $n = 1$ , **2c**;  $L = 2-(C_4H_3N-2'-CH=N)CH_2C_6H_4-2-OMe$ ,  $x = 3$ ,  $n = 0$ , **2d**;  $L = 2-(C_4H_3N-2'-CH=N)C_2H_4NPh$ ,  $x = 2$ ,  $n = 0$ , **4a**] were prepared and characterized by elemental analysis, NMR spectroscopy, and by X-ray crystallography for **2a** and **4a**. In the solid state, **2a** and **4a** are monomeric with the pyrrolide-imino-amine adopting a *mer*-configuration. Upon activation with methylaluminoxane (MAO), all Zr(IV) precatalysts were active in ethylene polymerization and exhibited high thermal stability operating effectively at 100 °C with activities up to 453 kg(PE).mol[Zr]<sup>-1</sup>.h<sup>-1</sup>. The high-density polyethylenes produced are strictly linear with melting temperatures in the range of 134–136 °C, and crystallinities varying from 56% to 70%.

## 1. Introduction

In the past few decades, the design and synthesis of *non*-metallocene olefin polymerization catalysts have drawn considerable attention in both academic and industrial fields largely due to their high performance in the production of polyolefin products.<sup>1</sup> Among the wide array of catalysts that have been used for this purpose, those ones based on Group 4 metals comprising bidentate,<sup>2</sup> tridentate,<sup>3</sup> and tetradentate<sup>4,5</sup> ligands incorporating *O*, *S*, *P*, and *N* donor atoms are the most frequently studied. Remarkable results have been achieved with Ti(IV) and Zr(IV) complexes supported by bis-ligated phenoxy-imine,<sup>2a-b,6</sup> ONNO-,<sup>4</sup> and OSSO-type bis(phenolate),<sup>5</sup> which are effective catalytic precursors for production of many important polyolefins, such as high-molecular-weight polyethylene, isotactic, and syndiotactic polypropylene. In addition, Group 4 metal-based catalysts bearing bi- and tridentate ligands bearing a pyrrolyl unit have been also successfully used to generate stable and highly active systems in ethylene polymerization.<sup>7</sup> For instance, Fujita *et al.* developed Ti(IV) complexes having two non-symmetric bidentate pyrrolide-imine chelate ligands (Chart 1) that, once activated with methylaluminoxane (MAO), generate highly active polymerization species (up to 14,100 kg(PE).mol(Ti)<sup>-1</sup> h<sup>-1</sup> at 25 °C).<sup>7a</sup>

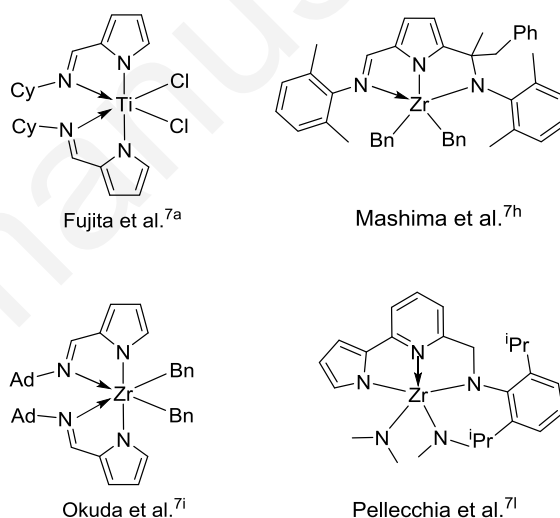


**Chart 1.** Selected examples of Group 4 complexes supported by pyrrolyl-based ligands applied in homopolymerization of ethylene.

In 2004, Mashima *et al.* reported a series of active amido-pyrrolyl Zr(IV) complexes (Chart 1) that, in combination with modified-methylaluminoxane (MMAO), exhibited high catalytic productivities (131,0–458,0 kg(PE).mol(Zr)<sup>-1</sup> h<sup>-1</sup> at 60–75 °C).<sup>7h</sup> Also, Okuda *et al.* described the synthesis of thermally robust dibenzyl Hf(IV) and Zr(IV) bearing substituted pyrrolide-imine complexes.<sup>7i</sup> Particularly, zirconium complexes [2-(RNCH)C<sub>4</sub>H<sub>3</sub>N]<sub>2</sub>ZrCl<sub>2</sub> (R = <sup>t</sup>Bu, 1-adamantyl) displayed a remarkably high ethylene polymerization productivity when combined with MAO (17,952–22,944 kg(PE).mol(Zr)<sup>-1</sup> h<sup>-1</sup> bar<sup>-1</sup> at 25 °C).

More recently, Pellecchia *et al.* reported the synthesis of a new Zr(IV) complex containing a amidomethyl-pyrrolide-pyridine tridentate ligand (Chart 1).<sup>7l</sup> Activation by Al<sup>i</sup>Bu<sub>2</sub>H / MAO resulted in a highly productive catalytic system, even at

<sup>a</sup> Laboratory of Molecular Catalysis, Instituto de Química, Universidade Federal do Rio Grande do Sul, Avenida Bento Gonçalves, 9500, RS, 91501-970 (Brazil). E-mail: osvaldo.casagrande@ufrgs.br

<sup>b</sup> Institut des Sciences Chimiques de Rennes, Centre de diffraction X, UMR 6226 CNRS-Université de Rennes 1, F-35042 Rennes Cedex, France

<sup>c</sup> Institut des Sciences Chimiques de Rennes, Organometallics: Materials and Catalysis Dept., UMR 6226 CNRS-Université de Rennes 1, F-35042 Rennes Cedex, France. E-mail: jean-francois.carpentier@univ-rennes1.fr

† Electronic Supplementary Information (ESI) available: Crystallographic data for **3b** and NMR data for zirconium complexes **2a–d** and **4a**. See DOI: 10.1039/x0xx00000x

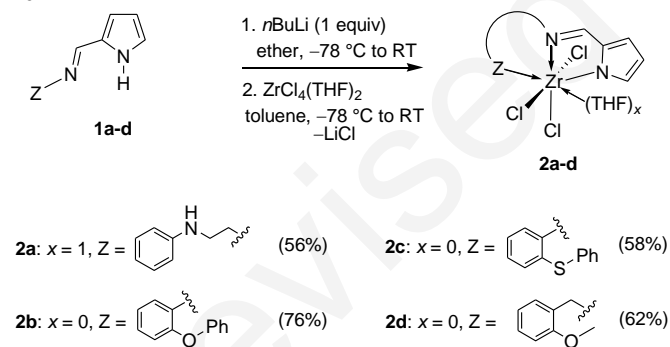
room temperature ( $1,840 \text{ kg(PE).mol(Zr)}^{-1} \text{ h}^{-1} \text{ bar}^{-1}$ ). Using the same activation system, this zirconium complex was able to polymerize propylene, affording isotactic polypropylene via an “enantiomorphic site” stereocontrol mechanism.

Inspired by these successful results, we have recently developed a series of pyrrolide-imino tridentate ligands with pendant *N*-, *O*- and *S*- donor group, and their Cr(III) and Ni(II) complexes. These precatalysts showed good activities in ethylene oligomerization upon MAO activation with high selectivities for production of  $\alpha$ -olefins.<sup>8</sup> As part of our continuing interest in developing catalytic systems using the pyrrolide-based ligands, the present contribution focuses on the synthesis of Zr(IV) complexes, and their application as catalysts for ethylene polymerization. Our aim was to explore the influence on catalytic performance of the donor side-arm and chelating mode within this series of ligands.

## 2. Results and discussion

### Synthesis and Characterization of Zirconium Complexes

The pyrrole-imino pro-ligands with pendant *N*-, *O* and *S*- donor groups (**1a-d**) were readily synthesized by Schiff base condensations between the corresponding primary amines and pyrrole-2-carboxaldehyde in refluxing methanol.<sup>8</sup> Treatment of **1a-d** with 1 equiv of *n*BuLi and then 1 equiv of  $\text{ZrCl}_4(\text{THF})_2$  yielded the corresponding Zr(IV) complexes **2a-d**, which were isolated as yellow or brown solids, in moderate to good yields (Scheme 1). These complexes are readily soluble in  $\text{CH}_2\text{Cl}_2$  and moderately soluble in acetonitrile and THF at room temperature. The identity of **2a-d** was established on the basis of combustion elemental analysis,  $^1\text{H}$  and  $^{13}\text{C}$  NMR spectroscopy, and single-crystal X-ray diffraction studies for **2a**.



**Scheme 1** Synthesis of zirconium complexes **2a-d**.

The room temperature  $^1\text{H}$  NMR spectra of zirconium complexes **2a-d** (Fig. S2, S4, S6, S8, respectively) in  $\text{CD}_2\text{Cl}_2$  showed no resonance in the region  $\delta$  9.40-9.81 ppm (ascribed to the pyrrole hydrogen), confirming the coordination of the pyrrolide group to the metal center. Additionally, the signals for the  $\text{CH}=\text{N}$  hydrogens were shifted downfield (0.03-0.37 ppm) vs. the corresponding resonance of the free pro-ligands, indicating the coordination of the imino nitrogen atom to

zirconium. Complex **2a** proved unstable in solution ( $\text{CD}_2\text{Cl}_2$ , THF) and decomposed to unknown products, preventing from collecting clean NMR spectra; however, diagnostic resonances for **2a** could be unambiguously identified (Fig. S2). In particular, the amine hydrogen resonance at  $\delta$  4.67 ppm was shifted downfield 0.69 ppm with respect to the one in the free ligand, further corroborating coordination of the amine group to the zirconium atom in solution.

Single crystals of **2a** suitable for an X-ray diffraction analysis were obtained in toluene at room temperature. The molecular geometry and atom-labeling scheme is shown in Figure 1.

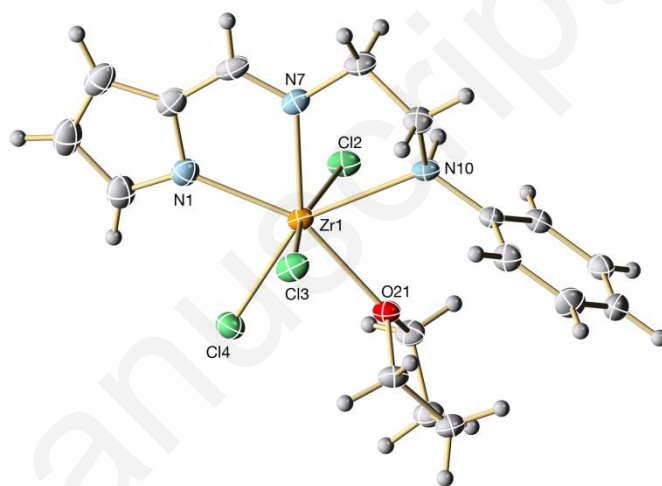


**Fig. 1** ORTEP drawing of  $[\text{Zr}\{2-(\text{C}_4\text{H}_3\text{N}-\text{CH}=\text{N})\text{C}_2\text{H}_4\text{NHPh}\}(\text{THF})\text{Cl}_3]$  (**2a**) (thermal ellipsoids drawn at the 30% probability level). Selected bond distances (Å) and angles (deg):  $\text{Zr}(1)-\text{N}(1) = 2.251(2)$ ,  $\text{Zr}(1)-\text{O}(21) = 2.2985(16)$ ,  $\text{Zr}(1)-\text{N}(7) = 2.3221(19)$ ,  $\text{Zr}(1)-\text{Cl}(2) = 2.4318(6)$ ,  $\text{Zr}(1)-\text{Cl}(3) = 2.4291(6)$ ,  $\text{Zr}(1)-\text{Cl}(4) = 2.4987(7)$ ,  $\text{Zr}(1)-\text{N}(10) = 2.526(2)$ .  $\text{N}(1)-\text{Zr}(1)-\text{O}(21) = 151.10(7)$ ,  $\text{N}(1)-\text{Zr}(1)-\text{N}(10) = 135.52(7)$ ,  $\text{N}(1)-\text{Zr}(1)-\text{N}(7) = 70.04(7)$ ,  $\text{N}(7)-\text{Zr}(1)-\text{N}(10) = 66.02(7)$ ,  $\text{O}(21)-\text{Zr}(1)-\text{N}(7) = 138.82(7)$ ,  $\text{N}(1)-\text{Zr}(1)-\text{Cl}(3) = 98.97(5)$ ,  $\text{O}(21)-\text{Zr}(1)-\text{Cl}(3) = 87.07(4)$ ,  $\text{N}(7)-\text{Zr}(1)-\text{Cl}(3) = 85.97(5)$ ,  $\text{N}(1)-\text{Zr}(1)-\text{Cl}(2) = 93.91(5)$ ,  $\text{O}(21)-\text{Zr}(1)-\text{Cl}(2) = 86.19(4)$ ,  $\text{N}(7)-\text{Zr}(1)-\text{Cl}(2) = 89.58(5)$ ,  $\text{Cl}(3)-\text{Zr}(1)-\text{Cl}(2) = 164.0(2)$ ,  $\text{N}(1)-\text{Zr}(1)-\text{Cl}(4) = 77.61(6)$ ,  $\text{O}(21)-\text{Zr}(1)-\text{Cl}(4) = 73.79(4)$ ,  $\text{N}(7)-\text{Zr}(1)-\text{Cl}(4) = 147.18(5)$ ,  $\text{Cl}(3)-\text{Zr}(1)-\text{Cl}(4) = 93.8(2)$ ,  $\text{Cl}(2)-\text{Zr}(1)-\text{Cl}(4) = 98.14(2)$ ,  $\text{O}21-\text{Zr}1-\text{N}10 = 72.95(6)$ ,  $\text{Cl}(3)-\text{Zr}(1)-\text{N}(10) = 84.69(5)$ ,  $\text{Cl}(2)-\text{Zr}(1)-\text{N}(10) = 79.46(5)$ ,  $\text{Cl}(4)-\text{Zr}(1)-\text{N}(10) = 146.73(5)$ .

Crystallographic data are summarized in Table 1. The solid-state molecular structure of **2a** revealed a seven-coordinate species, in which the Zr(IV) lies in a pseudo-pentagonal bipyramidal environment (Figure 1). The zirconium center bears  $\kappa^3\text{-N,N,N-}$  chelating pyrrolide-imino-amine ligand in a tridentate meridional fashion, with the three chloride ligands and the THF molecule completing the coordination sphere. The axial positions are occupied by two chlorides, with  $\text{Cl}(3)-\text{Zr}(1)-\text{Cl}(2) = 164.0(2)^\circ$ , and the sum of the equatorial  $\text{N}(1)-\text{Zr}(1)-\text{N}(7)$ ,  $\text{N}(1)-\text{Zr}(1)-\text{Cl}(4)$ ,  $\text{O}(21)-\text{Zr}(1)-\text{Cl}(4)$ , and  $\text{N}(7)-\text{Zr}(1)-\text{N}(10)$  bond angles is  $360.4^\circ$ . The

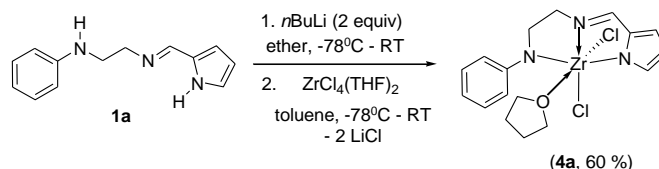
Zr(1)–N<sub>pyrrolyl</sub> (2.251(2) Å) and Zr(1)–N<sub>imido</sub> (2.322(2) Å) bond distances are comparable with those found in similar Zr(IV) complexes which contain imido-pyrrolide ligands.<sup>9</sup>

**Table 1** Crystal data and structure refinement for **2a** and **4a**.

	<b>2a</b>	<b>4a</b>
Molecular formula	C <sub>17</sub> H <sub>22</sub> Cl <sub>3</sub> N <sub>3</sub> OZr	C <sub>17</sub> H <sub>21</sub> Cl <sub>2</sub> N <sub>3</sub> OZr
Formula weight (g mol <sup>-1</sup> )	481.95	445.49
T (K)	150(2)	150(2)
Crystal system	monoclinic	monoclinic
Space group	<i>P</i> 2 <sub>1</sub> / <i>a</i>	<i>P</i> 2 <sub>1</sub> / <i>a</i>
<i>a</i> (Å)	7.4895(4)	15.6351(4)
<i>b</i> (Å)	28.0652(15)	7.2529(2)
<i>c</i> (Å)	9.2016(6)	16.5555(3)
$\alpha$ (°)	90	90
$\beta$ (°)	91.862(2)	95.5510(10)
$\gamma$ (°)	90	90
<i>V</i> (Å <sup>3</sup> )	1933.10(19)	1868.59(8)
<i>Z</i>	4	4
$\rho_{\text{calcd}}$ (g cm <sup>-3</sup> )	1.656	1.584
$\mu$ (mm <sup>-1</sup> )	0.994	0.883
<i>F</i> (000)	976	904
Crystal size (mm)	0.16 x 0.13 x 0.08	0.40 x 0.30 x 0.24
$\theta$ range (°)	3.08 to 27.48	3.1 to 27.47
Limiting indices ( <i>h</i> , <i>k</i> , <i>l</i> )	–9 ≤ <i>h</i> ≤ 8 –32 ≤ <i>k</i> ≤ 36 –11 ≤ <i>l</i> ≤ 11	–20 ≤ <i>h</i> ≤ 20 –9 ≤ <i>k</i> ≤ 9 –19 ≤ <i>l</i> ≤ 21
Reflections collected	17213	14297
Reflections unique ( <i>R</i> <sub>int</sub> )	4429 (0.0442)	4264 (0.0247)
Completeness to $\theta_{\text{max}}$ (%)	99.8	99.3
Data / restraints / param.	4429 / 0 / 226	4264 / 0 / 217
Min. and max. transmission	0.924 and 0.829	0.809 and 0.692
<i>R</i> <sub>1</sub> [ <i>I</i> > 2 $\sigma$ ( <i>I</i> )]	0.0323	0.0279
<i>wR</i> <sub>2</sub> [ <i>I</i> > 2 $\sigma$ ( <i>I</i> )]	0.0654	0.0717
<i>R</i> <sub>1</sub> (all data)	0.0458	0.0342
<i>wR</i> <sub>2</sub> (all data)	0.0712	0.0669
Largest diff. peak and hole (e Å <sup>-3</sup> )	0.497 and –0.434	0.835 and –0.935

Recrystallization of **2b** in toluene at room temperature afforded a few yellow crystals of [Zr{2-(C<sub>4</sub>H<sub>3</sub>N-2-CH=N)C<sub>6</sub>H<sub>4</sub>-2-OPh}<sub>2</sub>Cl<sub>2</sub>] (**3b**) (ca. 6% yield), and a large amount of unidentified products. The formation of bis(ligand) complex **3b** can be rationalized in terms of a ligand redistribution reaction. (For the X-ray structure of **3b**, please see ESI, Table S1 and Fig S1)

Double deprotonation of **1a** with 2 equiv of *n*BuLi in ether, followed by treatment with 1 equiv of ZrCl<sub>4</sub>(THF)<sub>2</sub> in toluene at –78 °C, afforded [Zr{2-(C<sub>4</sub>H<sub>3</sub>N-2-CH=N)C<sub>2</sub>H<sub>4</sub>NPh}(THF)Cl<sub>2</sub>] (**4a**) as a yellow solid in 60% yield (Scheme 2). This zirconium complex was characterized by <sup>1</sup>H and <sup>13</sup>C NMR spectroscopy, elemental analysis, and an X-ray diffraction study.



**Scheme 2** Synthesis of zirconium complex **4a**.

The <sup>1</sup>H and <sup>13</sup>C NMR spectra (Fig. S10 and S11, respectively) are consistent with the formation of **4a**. Two distinct sets of resonances were observed (6:1 ratio), which we assigned to possible isomers (differing by the relative positioning of N,Cl and O(THF) ligands). The absence of the hydrogen signals ascribed to the N-H groups of the pyrrole and amine groups indicated actual coordination of the pyrrolide-imino-amide to zirconium as a dianionic ligand. In the <sup>13</sup>C NMR spectrum of **4a**, the resonance of the CH=N imine carbon ( $\delta$  159.83 ppm for the major isomer; 159.61 ppm for the minor isomer) is shifted downfield compared to that of the free ligand ( $\delta$  153.40 ppm), which is indicative of imine coordination to the Zr(IV) center.

Single crystals of **4a** suitable for an X-ray diffraction analysis were obtained by recrystallization from a toluene solution at room temperature. Crystallographic data are summarized in Table 1, and selected important bond distances and angles are given in Figure 2.

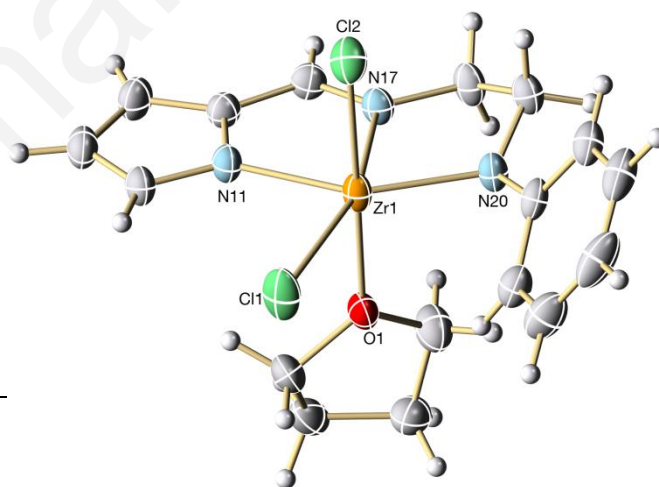


**Fig. 2** ORTEP drawing of [Zr{2-(C<sub>4</sub>H<sub>3</sub>N-2-CH=N)C<sub>2</sub>H<sub>4</sub>NPh}(THF)Cl<sub>2</sub>] (**4a**). Ellipsoids are drawn at the 30% probability level. Selected bond distances (Å) and angles (deg): Zr(1)–N(20) = 2.0783(16), Zr(1)–N(11) = 2.1969(17), Zr(1)–O(1) = 2.2363(15), Zr(1)–N(17) = 2.2844(17), Zr(1)–Cl(1) = 2.4684(6), Zr(1)–Cl(2) = 2.4464(6). N(20)–Zr(1)–N(11) = 140.50(7), N(20)–Zr(1)–Cl(1) = 129.45(5), N(17)–Zr(1)–Cl(2) = 92.14(5), N(20)–Zr(1)–O(1) = 89.17(6), N(11)–Zr(1)–O(1) = 85.99(6), N(20)–Zr(1)–N(17) = 70.10(6), N(11)–Zr(1)–N(17) = 70.48(6), O(1)–Zr(1)–N(17) = 86.48(6), N(20)–Zr(1)–Cl(2) = 91.33(5), N(11)–Zr(1)–Cl(2) = 92.77(5), O(1)–Zr(1)–Cl(2) = 178.55(4), N(11)–Zr(1)–Cl(1) = 89.30(5), O(1)–Zr(1)–Cl(1) = 85.94(4), N(17)–Zr(1)–Cl(1) = 158.85(4), Cl(2)–Zr(1)–Cl(1) = 94.78(2).

In the solid state, **4a** features a monomeric structure with pyrrolide-imino-amine ligand acting as a dianionic tridentate ligand. The coordination geometry around the metal center is distorted octahedral with the equatorial plane defined by the three nitrogen atoms of the ligand [ $N(20)-Zr(1)-N(11) = 140.50(7)^\circ$ ,  $N(20)-Zr(1)-N(17) = 70.10(6)^\circ$ ,  $N(11)-Zr(1)-N(17) = 70.48(6)^\circ$ ] and one chlorine atom [ $N(20)-Zr(1)-Cl(1) = 129.45(5)^\circ$ ,  $N(17)-Zr(1)-Cl(1) = 158.85(4)^\circ$ ,  $N(11)-Zr(1)-Cl(1) = 89.30(5)^\circ$ ]. The  $Zr-N_{\text{amine}}$  bond distance ( $2.078(2) \text{ \AA}$ ) is shorter than the  $Zr-N_{\text{imino}}$  distance in **2a** ( $2.526(2) \text{ \AA}$ ) indicating that the  $N(20)$  atom formed a  $\sigma$ -bond with Zr. The two chloride ligands are located *cis* to each other [ $Cl(2)-Zr(1)-Cl(1) = 94.78(2)^\circ$ ] which is favorable for ethylene polymerization. The  $Zr(1)-Cl(1)$  bond [*trans* to the imino nitrogen,  $2.4684(6) \text{ \AA}$ ] is longer than  $Zr(1)-Cl(2)$  (*trans* to O atom) [ $2.4464(6) \text{ \AA}$ ], as the result of the *trans* influence.

To compare the steric properties of **2a** and **4a**, topographic steric maps were generated using the SambVca 2 Web application recently developed by Cavallo *et al* (Figure 3).<sup>10</sup> It is interesting to note that the same ligand can shape different steric maps. Thus, in **2a**, the higher coordination number and the coordination of the pyrrolide-imino-amine ligand as a monoanionic tridentate ligand resulted in a lower percent buried volume ( $\%V_{\text{Bur}}$ ) with respect to **4a**. The steric map of **4a** clearly shows significant increase in steric protection around the Zr metal center after formation of  $\sigma$ -bond with the -NPh moiety.

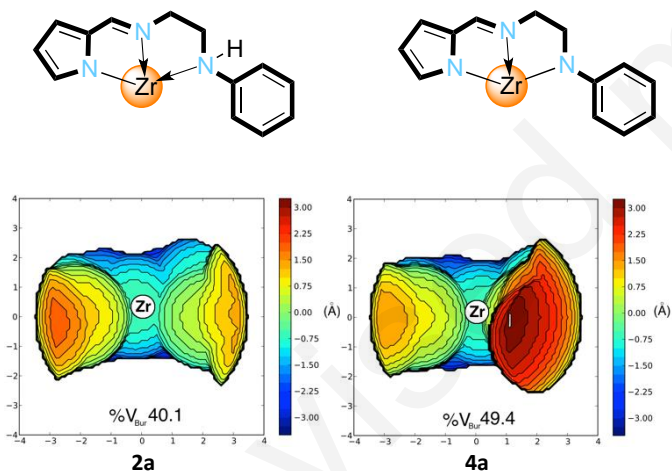


**Fig. 3** Steric maps of zirconium complexes bearing pyrrolide-imino-amine (**2a**) and amide (**4a**) ligands.

### Ethylene polymerization Studies

Ethylene homopolymerization was investigated using zirconium complexes **2a-d** and **4a** in toluene at  $60^\circ\text{C}$ , 5 bar constant ethylene pressure, and MAO as cocatalyst. Typical results are collected in Table 2. All experiments were at least duplicated, yielding reproducible results within  $\pm 10\%$ . Initial studies, carried out at  $60^\circ\text{C}$  with  $[Al]/[Zr] = 500$ , showed that these catalyst systems were moderately active, producing

high-density polyethylene (HDPE) with melting temperatures ( $T_m$ ) in the range of  $133\text{--}136^\circ\text{C}$ , and crystallinities varying from 31% to 70%. The HDPE samples displayed very low solubility in hot *o*-dichlorobenzene ( $140^\circ\text{C}$ ), making impossible gel permeation chromatography (GPC) analysis and suggesting high molecular weights.<sup>11</sup>

The polymerization results showed that coordination of **1a** either as mono- or dianionic mode does not provide any significant effect on the activity. In fact, the catalytic systems based on **2a** and **4a** gave similar productivities of 22 and 23  $\text{kg(PE).mol(Zr)}^{-1}.\text{h}^{-1}$ , respectively. It is actually possible that deprotonation of the NH moiety in **2a** occurs upon activation with excess MAO. On the other hand, complexes **2b** and **2c**, with a pendant *O*- and *S*-donor group generated catalyst systems much more active than **2a** (compare entries 1-3). This observation suggests that the presence of a more rigid pendant group ( $-\text{C}_6\text{H}_4\text{EPH}$ ,  $\text{E} = \text{O}, \text{S}$ ) can promote a better stabilization of the catalytically active species, and thus improve the catalyst performance. The highest productivity observed for **2b** ( $166 \text{ kg(PE).mol(Zr)}^{-1}.\text{h}^{-1}$  at  $60^\circ\text{C}$ ), compares well with other zirconium complexes bearing pyrrolide ligands,<sup>7</sup> but definitively do not compete with Okuda's system.<sup>71</sup>

By comparing **2d** and **2b**, increasing the length of the spacer between the central imine and the ether donor group by one carbon decreases the catalytic activity by a factor of 1.8. This is in line with the above results and strongly suggests a correlation between the ligand stereorrigidity and activity of catalyst. Thus, the coordination of a more flexible ligand (**1d**) to the zirconium atom may generate a less stable catalytic species. A similar trend has been observed for imino-phenolate titanium complexes bearing *O*-phenyl and *O*-methyl pendant groups.<sup>12</sup>

Influences of the MAO loading, reaction time, and reaction temperature on ethylene polymerization were investigated in detail with complexes **2b** and **4a**. The results are summarized in Table 2. The MAO loading has a significant influence on the activity of **2b**. Thus, increasing the  $[Al]/[Zr]$  molar ratio from 250 to 500 led to an enhancement of the ethylene polymerization productivity (from 100 to  $166 \text{ kg(PE).mol(Zr)}^{-1}.\text{h}^{-1}$ ). Use of higher MAO loading ( $[Al]/[Zr] = 2000$ ) did not significantly affect the productivity ( $175 \text{ kg(PE).mol(Zr)}^{-1}.\text{h}^{-1}$ ). However, further increasing the amount of MAO ( $[Al]/[Zr] = 2000$ ) rendered a slightly less active system. This reduction can be tentatively associated to a more difficult coordination of ethylene to the metal center due to the presence of higher MAO (and hence  $\text{AlMe}_3$ ) loading. Yet, we cannot discard the possibility that  $\text{AlMe}_3$  (TMA) present in MAO may coordinate to the active species, to yield inactive catalyst.<sup>13</sup>

To assess the deactivation process, a lifetime study of the **4a**/MAO catalytic system was conducted over 5, 15 and 30 min at  $60^\circ\text{C}$  with an optimized  $[Al]/[Zr]$  molar ratio of 1000 (entries 10-12). As can be seen in Figure 4, the relationship between reaction time and polymer yield indicates that the **4a**/MAO catalytic system actually undergoes complete deactivation shortly after 5 min.

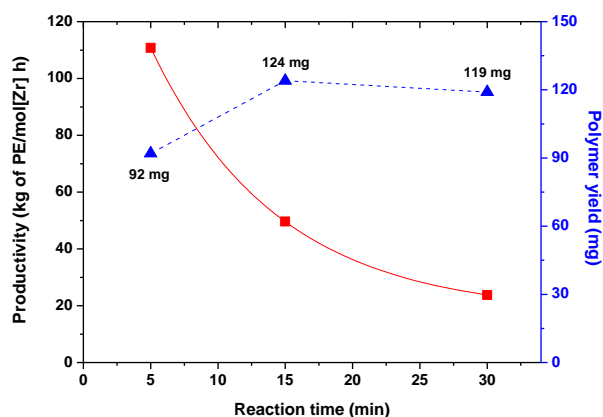


**Fig. 4** Lifetime graph of ethylene polymerization for precatalyst **4a** (60 °C, 10  $\mu$ mol catalyst,  $P_{C_2H_4}$  = 5 bar,  $[Al]/[Zr]$  = 1,000).

The catalytic performance of precatalyst **4a** was also studied by varying the temperature. Increasing the polymerization temperature from 60 °C to 100 °C led to an increase of the productivity from 111 to 453 kg(PE).mol(Zr)<sup>-1</sup>.h<sup>-1</sup>. A similar result was also found for **2b**, where the activity at 100 °C is *ca* 1.6 times higher than that at 60 °C (compare entries 5 and 7). Overall, these results indicate a key role of this class of pyrrolide-imino-amine(amide)/ether ligands in the thermal stabilization of the active catalytic species.

**Table 2** Ethylene Polymerization with **2a-d**/MAO and **4a**/MAO catalytic systems.<sup>a</sup>

entry	cat	[Al]/[Zr]	Temp (°C)	Time (min)	$m_{Pol}$ (g)	Productivity <sup>b</sup>	$T_m$ (°C)	$X$ (%)
1	<b>2a</b>	500	60	15	0.058	23	135	71
2	<b>2b</b>	500	60	15	0.416	166	136	66
3	<b>2c</b>	500	60	15	0.180	72	134	32
4	<b>2d</b>	500	60	15	0.230	92	134	31
5	<b>4a</b>	500	60	15	0.055	22	134	54
6	<b>2b</b>	250	60	15	0.257	103	134	44
7	<b>2b</b>	1000	60	15	0.437	175	136	59
8	<b>2b</b>	2000	60	15	0.356	142	131	38
9	<b>2b</b>	1000	100	15	0.712	286	133	41
10	<b>4a</b>	1000	60	5	0.092	111	135	47
11	<b>4a</b>	1000	60	15	0.124	50	134	45
12	<b>4a</b>	1000	60	30	0.119	24	132	43
13	<b>4a</b>	1000	80	5	0.200	230	134	49
14	<b>4a</b>	1000	100	5	0.394	453	133	52

<sup>a</sup> Reaction conditions: toluene = 90 mL,  $[Zr]$  = 10  $\mu$ mol, P(ethylene) = 5 bar (kept constant), MAO as cocatalyst. The results shown are representative of at least duplicated experiments. The results shown are representative of at least duplicated experiments, yielding reproducible results within  $\pm 10\%$ . <sup>b</sup> in kg (PE).mol(Zr)<sup>-1</sup>.h<sup>-1</sup>. <sup>c</sup> Crystallinity calculated as  $(\Delta H_f/\Delta H_{f\alpha}) \times 100$ , with  $\Delta H_{f\alpha}$  = 286.6 J g<sup>-1</sup>.

## Conclusions

We have described the synthesis of a new set of Zr(IV) complexes bearing pyrrolide-imino tridentate ligands with pendant *N*-, *O*- and *S*-donor groups. The ability of pyrrolide-imino-amine/amide ligand to act as a mono- or dianionic ligand enabled the preparation of two different zirconium

complexes. Complexes **2a-d** and **4a** are catalyst precursors for the polymerization of ethylene producing high-density polyethylenes. The complete insolubility of these PEs in common solvents suggests that these polymers may have very high molecular weights. The coordination of pyrrolide-imino-amine ligand either as mono- or dianionic mode does not provide any significant effect on the activity, suggesting that

**2a** and **4a** might be equivalent precursors toward the same active species. On the other hand, the much higher activity observed in the presence of a more rigid pendant group (-C<sub>6</sub>H<sub>4</sub>OPh) as in **2b** suggests a better stabilization of the catalytically active species. The optimization study showed that this class of catalysts displayed better activities at high MAO loading ([Al]/[Zr] = 1000) and high polymerization temperature (100 °C). The latter observation indicates that pyrrolide-imino-amine/amide/ether ligands play a significant role in the thermal stabilization of the active catalytic species. However, this class of ligands is not able to guarantee a long lifetime, as the catalyst undergoes almost complete deactivation shortly after 5 min. Further studies are underway in our laboratories to investigate the catalytic behavior of this class of zirconium complexes in ethylene/1-hexene copolymerization and the results will be reported in due course.

## Experimental

### General Procedures

All manipulations involving air- and/or moisture-sensitive compounds were carried out in an MBraun glovebox or under dry argon using standard Schlenk techniques. Toluene, THF, and hexane were dried over a Braun MB-SPS-800 solvent purification system. Other solvents were dried from the appropriate drying agents under argon before use. ZrCl<sub>4</sub>(THF)<sub>2</sub> was purchased from Sigma-Aldrich and used as received. Ethylene (White Martins Co.) and argon were deoxygenated and dried through BTS columns (BASF) and 3A activated molecular sieves prior to use. 2-(C<sub>4</sub>H<sub>4</sub>N-2'-CH=N)C<sub>2</sub>H<sub>4</sub>NHPh (**1a**), 2-(C<sub>4</sub>H<sub>4</sub>N-2'-CH=N)C<sub>6</sub>H<sub>4</sub>-2-OPh (**1b**), 2-(C<sub>4</sub>H<sub>4</sub>N-2'-CH=N)C<sub>6</sub>H<sub>4</sub>-2-SPh (**1c**), 2-(C<sub>4</sub>H<sub>4</sub>N-2'-CH=N)C<sub>6</sub>H<sub>4</sub>-2-OCH<sub>3</sub> (**1d**) were prepared by following literature procedures.<sup>8</sup> MAO (AXION® CA 1310, 10 wt.-% solution in toluene) was used as received. NMR spectra were recorded on a Bruker AM-500 spectrometer. <sup>1</sup>H and <sup>13</sup>C NMR chemical shifts are reported in ppm vs. SiMe<sub>4</sub> and were determined by reference to the residual solvent peaks. Elemental analyses were performed by the Analytical Central Service of the Institute of Chemistry-USP (Brazil) and are the average of two independent determinations. Melting temperatures were determined by differential scanning calorimetry (DSC) with a Thermal Analysis Instruments DSC-Q20 using a heating rate of 10 °C min<sup>-1</sup> after twice previous heating to 180 °C and cooling to 40 °C at 10 °C min<sup>-1</sup>.

### Synthesis of the Zr(IV) Complexes

**[Zr{2-(C<sub>4</sub>H<sub>3</sub>N-2-CH=N)C<sub>2</sub>H<sub>4</sub>NHPh}(THF)Cl<sub>3</sub>] (2a).** To a stirred solution of **1a** (0.167 g, 0.78 mmol) in dried diethyl ether (10 mL) at -78 °C was added dropwise 1 equiv of *n*-butyllithium (0.340 mL of a 2.3 M solution in diethyl ether, 0.78 mmol). The resulting solution was allowed to stir for 2 h at room temperature and then the solvent was removed under vacuum to give a light pink solid residue. This solid was suspended in toluene (10 mL), cooled to -78 °C, and added dropwise to a

solution of ZrCl<sub>4</sub>(THF)<sub>2</sub> (0.294 g, 0.78 mmol) in toluene (10 mL). The reaction mixture was stirred for 24 h at room temperature, filtered by cannula and the resulting solution was concentrated (ca. 2 mL) to give **2a** as yellow crystals, some of which proved suitable for X-ray diffraction studies (0.210 g, 56%). **Complex 2a** proved unstable in solution (CD<sub>2</sub>Cl<sub>2</sub>, THF) and decomposed to unknown products, preventing from collecting clean NMR spectra; however, diagnostic resonances for **2a** could be unambiguously identified: <sup>1</sup>H NMR (500 MHz, CD<sub>2</sub>Cl<sub>2</sub>, 25 °C): δ 8.14 (s, 1H, N=CH), 7.47-7.37 (m, 5H, Ar-H), 6.88 (s, 1H, 5-pyr), 6.70 (s, 1H, 3-pyr), 6.31 (s, 1H, 4-pyr), 4.67 (s, 1H, NH), 4.11 (t, <sup>3</sup>J<sub>HH</sub> = 5.7 Hz, 2H, CH<sub>2</sub>), 3.82 (s, OCH<sub>2</sub>CH<sub>2</sub>), 3.75 (t, <sup>3</sup>J<sub>HH</sub> = 5.7 Hz, 2H, CH<sub>2</sub>), 1.78 (s, 2H, OCH<sub>2</sub>CH<sub>2</sub>). <sup>13</sup>C{<sup>1</sup>H} NMR (125 MHz, CDCl<sub>3</sub>, 25 °C): δ 160.33 (C=N), 146.99 (quat. C<sub>aro</sub>), 138.89 (quat. C<sub>pyr</sub>), 129.87 (C<sub>pyr</sub>), 122.46 122.16, 120.57, 118.41, 113.33 (C<sub>aro</sub>), 112.99 112.35 (C<sub>pyr</sub>), 56.27 (OCH<sub>2</sub>CH<sub>2</sub>), 51.55 (=N-CH<sub>2</sub>CH<sub>2</sub>), 42.84 (=N-CH<sub>2</sub>CH<sub>2</sub>), 25.85 (OCH<sub>2</sub>CH<sub>2</sub>). Anal. Calcd. for C<sub>17</sub>H<sub>22</sub>Cl<sub>3</sub>ZrN<sub>3</sub>O: C: 42.36, H: 4.60, N: 8.72. Found: C: 42.12, H: 4.41, N: 8.54.

**[Zr{2-(C<sub>4</sub>H<sub>3</sub>N-2-CH=N)C<sub>6</sub>H<sub>4</sub>-2-OPh}Cl<sub>3</sub>] (2b).** This complex was prepared as described above for **2a**, starting from **1b** (0.203 g, 0.76 mmol), 1 equiv of *n*-butyllithium (0.33 mL of a 2.3 M solution in diethyl ether, 0.76 mmol) and ZrCl<sub>4</sub>(THF)<sub>2</sub> (0.286 g, 0.76 mmol) to give **2b** as a brown solid (0.265 g, 76%). <sup>1</sup>H NMR (500 MHz, CD<sub>2</sub>Cl<sub>2</sub>, 25 °C): δ 8.48 (s, 1H, N=C-H), 7.34-6.97 (m, 11H, Ar-H + 3-pyr + 5-pyr), 6.37 (s, 1H, 4-pyr). <sup>13</sup>C{<sup>1</sup>H} NMR (125 MHz, CDCl<sub>3</sub>, 25 °C): δ 163.22 (quat. OCPH), 158.30 (C=N), 149.79 (quat. C<sub>aro</sub>), 138.53 (quat. C<sub>aro</sub>), 130.41 (quat. C<sub>pyr</sub>), 128.72, 128.34, 125.16, 124.21, 123.19, 120.50, 119.17 (C<sub>aro</sub>), 118.34, 118.02, 112.10 (C<sub>pyr</sub>). Anal. Calcd. for C<sub>17</sub>H<sub>13</sub>Cl<sub>3</sub>ZrN<sub>2</sub>O: C: 44.50, H: 2.86, N: 6.10. Found: C: 44.05, H: 2.76, N: 5.89.

**[Zr{2-(C<sub>4</sub>H<sub>3</sub>N-2-CH=N)C<sub>6</sub>H<sub>4</sub>-2-SPh}(THF)Cl<sub>3</sub>] (2c).** This complex was prepared as described above for **2a**, starting from **1c** (0.150 g, 0.54 mmol), 1 equiv of *n*-butyllithium (0.23 mL of a 2.3 M solution in diethyl ether, 0.54 mmol) and ZrCl<sub>4</sub>(THF)<sub>2</sub> (0.203 g, 0.54 mmol) to give **2c** as a white solid (0.149 g, 58%). <sup>1</sup>H NMR (400 MHz, CD<sub>2</sub>Cl<sub>2</sub>, 25 °C): δ 8.06 (s, 1H, CH=N), 7.63-7.22 (m, 11H, Ar-H + 3-pyr + 5-pyr), 6.51 (s, 1H, 4-pyr). <sup>13</sup>C{<sup>1</sup>H} NMR (125 MHz, CDCl<sub>3</sub>, 25 °C): δ 149.76 (quat. C<sub>aro</sub>), 149.37 (C=N), 138.30, 137.71 (quat. C<sub>aro</sub>), 134.78 (quat. C<sub>pyr</sub>), 134.08, 132.66, 131.00, 129.92, 129.47, 127.78 (C<sub>aro</sub>), 124.53, 123.58, 115.20 (C<sub>pyr</sub>). Anal. Calcd. for C<sub>21</sub>H<sub>21</sub>Cl<sub>3</sub>ZrN<sub>2</sub>OS: C: 46.11, H: 3.87, N: 5.12. Found: C: 46.40, H: 4.17, N: 4.83.

**[Zr{2-(C<sub>4</sub>H<sub>3</sub>N-2-CH=N)CH<sub>2</sub>C<sub>6</sub>H<sub>4</sub>-2-OMe}Cl<sub>3</sub>] (2d).** This complex was prepared as described above for **2a**, starting from **1d** (0.180 g, 0.84 mmol), 1 equiv of *n*-butyllithium (0.37 mL of a 2.3 M solution in diethyl ether, 0.84 mmol) and 1 equiv of ZrCl<sub>4</sub>(THF)<sub>2</sub> (0.316 g, 0.84 mmol) to give **2d** as a pale brown solid (0.214 g, 62%). <sup>1</sup>H NMR (400 MHz, CD<sub>2</sub>Cl<sub>2</sub>, 25 °C): δ 7.95 (s, 1H, CH=N), 7.49-7.34 (m, 4H, Ar-H), 6.95-6.91 (m, 2H, Ar-H + 5-pyr + 3-pyr), 6.44 (s, 1H, 4-pyr), 4.82 (s, 2H, CH<sub>2</sub>), 3.84 (s, 3H, CH<sub>3</sub>). <sup>13</sup>C NMR (100 MHz, CD<sub>2</sub>Cl<sub>2</sub>, 25 °C): δ 158.47 (C=N), 152.55 (quat. OCPH), 148.91 (quat. C<sub>pyr</sub>), 145.18, 136.21, 131.85, 131.61 (C<sub>aro</sub>) 122.80 (quat. C<sub>aro</sub>), 121.47 (C<sub>pyr</sub>), 114.55 (C<sub>aro</sub>), 111.34, 111.30 (C<sub>pyr</sub>), 56.12 (CH<sub>2</sub>), 51.61 (CH<sub>3</sub>). Anal. Calcd. for C<sub>13</sub>H<sub>13</sub>Cl<sub>3</sub>ZrN<sub>2</sub>O: C: 38.01, H: 3.19, N: 6.82. Found: C: 37.45, H: 3.01, N: 6.61.

**[Zr{2-(C<sub>4</sub>H<sub>3</sub>N-2-CH=N)C<sub>2</sub>H<sub>4</sub>NPh}(THF)Cl<sub>2</sub>] (4a).** This complex was prepared as described above for **2a**, starting from **1a** (0.170 g, 0.78 mmol), 2 equiv of *n*-butyllithium (0.820 mL of a 2.3 M solution in diethyl ether, 1.87 mmol) and 1 equiv of ZrCl<sub>4</sub>(THF)<sub>2</sub> (0.294 g, 0.78 mmol) to give **4a** as a yellow solid (0.251 g, 60%). Two sets of resonances were observed in CD<sub>2</sub>Cl<sub>2</sub>, assigned to two isomers in a 6:1 ratio. <sup>1</sup>H NMR (500 MHz, CD<sub>2</sub>Cl<sub>2</sub>, 25 °C) major signals: δ 8.28 (s, 1H, N=C-H), 7.61-7.56 (m, 4H, Ar-H + 5-pyrrole), 7.30 (d, <sup>2</sup>J<sub>HH</sub> = 7.3 Hz, 2H, Ar-H), 6.87 (d, <sup>2</sup>J<sub>HH</sub> = 2.6 Hz, 1H, 3-pyrrole), 6.35 (s, 1H, 4-pyrrole), 4.18 (t, <sup>3</sup>J<sub>HH</sub> = 5.9 Hz, 2H, =N-CH<sub>2</sub>CH<sub>2</sub>), 4.12 (t, <sup>3</sup>J<sub>HH</sub> = 5.9 Hz, 2H, =N-CH<sub>2</sub>CH<sub>2</sub>), 3.94 (s, 4H, OCH<sub>2</sub>CH<sub>2</sub>), 1.80 (s, 4H, OCH<sub>2</sub>CH<sub>2</sub>); minor signals (all of them could not be identified as they overlap with the major set of resonances): δ 8.24 (s, 1H, N=C-H), 6.98 (d, 1H, 3-pyrrole), 6.40 (s, 1H, 4-pyrrole), 4.14 (t, <sup>3</sup>J<sub>HH</sub> = 6.0 Hz, 2H, =N-CH<sub>2</sub>CH<sub>2</sub>). <sup>13</sup>C{<sup>1</sup>H} NMR (125 MHz, CDCl<sub>3</sub>, 25 °C) major signals: δ 159.83 (C=N), 147.54 (quat. C<sub>aro</sub>), 140.43 (quat. C<sub>pyr</sub>), 138.86 (C<sub>aro</sub>), 130.36 (C<sub>pyr</sub>), 121.95, 118.93 (C<sub>aro</sub>), 115.77, 113.81 (C<sub>pyr</sub>), 56.19 (OCH<sub>2</sub>CH<sub>2</sub>), 55.77 (=N-CH<sub>2</sub>CH<sub>2</sub>), 55.23 (=N-CH<sub>2</sub>CH<sub>2</sub>), 25.33 (OCH<sub>2</sub>CH<sub>2</sub>); minor signals (all of them could not be identified as they overlap with the major set of resonances): δ 159.61 (C=N), 144.59 (quat. C<sub>aro</sub>), 143.91 (quat. C<sub>pyr</sub>), 137.96 (C<sub>aro</sub>), 129.87 (C<sub>pyr</sub>), 120.21, 117.38 (C<sub>aro</sub>), 112.59, 111.92 (C<sub>pyr</sub>). Anal. Calcd. for C<sub>17</sub>H<sub>21</sub>Cl<sub>2</sub>ZrN<sub>3</sub>O: C: 45.83, H: 4.75, N: 9.43. Found: C: 45.22, H: 4.68, N: 9.27.

#### General polymerization procedure

Ethylene polymerization runs were performed in a 250 mL double-walled stainless Parr reactor equipped with mechanical stirring, internal temperature control and continuous feed of ethylene. The Parr reactor was dried in an oven at 120 °C for 5 h prior to each run, and then cooled under vacuum for 30 min. A typical reaction was performed by introducing toluene (90 mL) and the proper amount of MAO into the reactor under an ethylene atmosphere. After 20 min, the toluene catalyst solution (10 mL, [Zr] = 10 μmol) was injected into the reactor under a stream of ethylene and then the reactor was immediately pressurized. Ethylene was continuously fed in order to maintain the desired ethylene pressure. Afterward, the reactor was depressurized and cooled to 25 °C. The polymer was precipitated using 20 mL of ethanol acidified with hydrochloric acid, under stirring for 30 min. After filtration and washing with small portions of acidic ethanol, then ethanol and water, the resulting material was dried in a vacuum oven at 60 °C for 12 h.

#### X-ray Diffraction Analyses

Suitable single-crystals of **2a** and **4a** were mounted onto a glass fiber using the "oil-drop" method. Selected bond lengths and angles are given in the Figure captions. Diffraction data were collected at 150(2) K using an APEXII Bruker-AXS diffractometer with graphite-monochromatized MoKα radiation (λ = 0.71073 Å). A combination of ω and φ scans was carried out to obtain at least a unique data set. The crystal structures were solved by direct methods, remaining atoms were located from difference Fourier synthesis followed by full-matrix least-squares refinement based on F<sup>2</sup> (programs

SIR97 and SHELXL-97) with the aid of the WINGX program. All non-hydrogen atoms were refined with anisotropic atomic displacement parameters. H atoms were finally included in their calculated positions. Crystal data and details of data collection and structure refinement can be obtained from the Cambridge Crystallographic Data Centre via [www.ccdc.cam.ac.uk/data\\_request/cif](http://www.ccdc.cam.ac.uk/data_request/cif) (CCDC 1561078 and 1561079).

#### Conflicts of interest

The authors declare no conflicts of interest.

#### Acknowledgements

This work was supported in part by the Petrobras S/A, FAPERGS/PRONEX, CAPES, French MESR, and CNRS. The authors are grateful to CAPES-COFECUB for joined Action 804/14.

#### Notes and references

- (a) T. Matsugi, T. Fujita, *Chem. Soc. Rev.* 2008, **37**, 1264. (b) D. Takeuchi, *Dalton Trans.* 2010, **39**, 311. (c) K. Nomura, S. Zhang, *Chem. Rev.* 2011, **111**, 2342. (d) J. Q. Wu, Y. S. Li, *Coord. Chem. Rev.* 2011, **255**, 2303. (e) V. C. Gibson, C. Redshaw, G. A. Solan, *Chem. Rev.*, 2007, **107**, 1745. (f) V. C. Gibson, S. K. Spitzmesser, *Chem. Rev.* 2003, **103**, 283. (g) S. D. Ittel, L. K. Johnson, M. Brookhart, *Chem. Rev.* 2000, **100**, 1169. (h) W.-H. Sun, H. Yang, Z. Li, Y. Li, *Organometallics* 2003, **22**, 3678. (i) M. Mitani, R. Furuyama, J. Mohri, J. Saito, S. Ishii, H. Terao, N. Kashiwa, T. Fujita, *J. Am. Chem. Soc.* 2002, **124**, 7888.
- (a) M. Mitani, J. Saito, S. Ishii, Y. Nakayama, H. Makio, N. Matsukawa, S. Matsui, J. Mohri, R. Furuyama, H. Terao, H. Bando, H. Tanaka, T. Fujita, *Chem. Rec.*, 2004, **4**, 137. (b) H. Makio, H. Terao, A. Iwashita, T. Fujita, *Chem. Rev.*, 2011, **111**, 2363. (c) J. Tian, P. D. Hustad, G. W. Coates, *J. Am. Chem. Soc.*, 2001, **123**, 5134. (d) S.-M. Yu, S. Mecking, *J. Am. Chem. Soc.*, 2008, **130**, 13204. (e) S.-F. Yua, T. Duan, L. Wang, X. Wei, X. Wang, W.-H. Sun, *Inorg. Chim. Acta*, 2017, **466**, 497.(f)
- (a) C. Redshaw, Y. Tang, *Chem. Soc. Rev.* 2012, **41**, 4484. (b) D. Peng, X. Yan, C. Yu, S. Zhang, X. Li, *Polym. Chem.*, 2016, **7**, 2601.

- 4 (a) E. Y. Tshuva, I. Goldberg, M. Kol, *J. Am. Chem. Soc.*, 2000, **122**, 10706. (b) S. Segal, I. Goldberg, M. Kol, *Organometallics*, 2005, **24**, 200. (c) A. Cohen, J. Kopilov, I. Goldberg, M. Kol, *Organometallics*, 2009, **28**, 1391.
- 5 (a) C. Capacchione, A. Proto, H. Ebeling, R. Mülhaupt, K. Möller, T. P. Spaniol, J. Okuda, *J. Am. Chem. Soc.*, 2003, **125**, 4964. (b) C. Capacchione, A. Proto, H. Ebeling, R. Mülhaupt, K. Möller, R. Manivannan, T. P. Spaniol, J. Okuda, *J. Mol. Catal. A: Chem.*, 2004, **213**, 137. (c) K. Beckerle, C. Capacchione, H. Ebeling, R. Manivannan, R. Mülhaupt, A. Proto, T. P. Spaniol, J. Okuda, *J. Organomet. Chem.*, 2004, **689**, 4636. (d) C. Capacchione, R. Manivannan, M. Barone, K. Beckerle, R. Centore, L. Oliva, A. Proto, A. Tuzi, T. P. Spaniol, J. Okuda, *Organometallics*, 2005, **24**, 2971. (e) K. Beckerle, R. Manivannan, T. P. Spaniol and J. Okuda, *Organometallics*, 2006, **25**, 3019. (f) S. Milione, C. Cuomo, C. Capacchione, C. Zannoni, A. Grassi, A. Proto, *Macromolecules*, 2007, **40**, 5638. (g) C. Capacchione, A. Avagliano, A. Proto, *Macromolecules*, 2008, **41**, 4573. (h) A. Proto, A. Avagliano, D. Saviello, C. Capacchione, *Macromolecules*, 2009, **42**, 6981. (i) A. Proto, A. Avagliano, D. Saviello, R. Ricciardi, C. Capacchione, *Macromolecules*, 2010, **43**, 5919. (j) C. Capacchione, D. Saviello, R. Ricciardi, A. Proto, *Macromolecules*, 2011, **44**, 7940. (k) C. Costabile, C. Capacchione, D. Saviello, A. Proto, *Macromolecules*, 2012, **45**, 6363. (l) A. Buonerba, M. Fienga, S. Milione, C. Cuomo, A. Grassi, A. Proto, C. Capacchione, *Macromolecules*, 2013, **46**, 8449. (m) A. Cohen, A. Yeori, I. Goldberg, M. Kol, *Inorg. Chem.*, 2007, **46**, 8114. (n) A. Ishii, T. Toda, N. Nakata, T. Matsuo, *J. Am. Chem. Soc.*, 2009, **131**, 13566. (o) A. Ishii, K. Asajima, T. Toda, N. Nakata, *Organometallics*, 2011, **30**, 2947. (p) N. Nakata, T. Toda, T. Matsuo, A. Ishii, *Macromolecules*, 2013, **46**, 6758.
- 6 J. Tian, P. D. Hustad, G. W. Coates, *J. Am. Chem. Soc.*, 2001, **123**, 5134.
- 7 (a) Y. Yoshida, S. Matsui, Y. Takagi, M. Mitani, M. Nitabaru, T. Nakano, H. Tanaka, T. Fujita, *Chem. Lett.*, 2000, 1270. (b) D. M. Dawson, D. A. Walker, M. Thornton-Pett, M. Bochmann, *J. Chem. Soc., Dalton Trans.*, 2000, 459. (c) Y. Yoshida, S. Matsui, Y. Takagi, M. Mitani, T. Nakano, H. Tanaka, N. Kashiwa, T. Fujita, *Organometallics*, 2001, **20**, 4793. (d) S. Matsui, T. P. Spaniol, Y. Takagi, Y. Yoshida, J. Okuda, *J. Chem. Soc., Dalton Trans.*, 2002, 4529. (e) Y. Yoshida, T. Nakano, H. Tanaka, T. Fujita, *Isr. J. Chem.*, 2002, **42**, 353. (f) Y. Yoshida, J. Saito, M. Mitani, Y. Takagi, S. Matsui, S. Ishii, T. Nakano, N. Kashiwa, T. Fujita, *Chem. Commun.*, 2002, 1298. (g) H. Tsurugi, T. Yamagata, K. Tani, K. Mashima, *Chem. Lett.*, 2003, **32**, 756. (h) H. Tsurugi, Y. Matsuo, T. Yamagata, K. Mashima, *Organometallics*, 2004, **23**, 2797. (i) S. Matsui, Y. Yoshida, Y. Takagi, T. P. Spaniol, J. Okuda, *J. of Organomet. Chem.*, 2004, **689**, 1155. (j) K. Vanka, Z. Xu, T. Ziegler, *Organometallics*, 2004, **23**, 2900. (k) Y. Yoshida, S. Matsui, T. Fujita, *J. Organomet. Chem.*, 2005, **690**, 4382. (l) L. Annunziata, D. Pappalardo, C. Tedesco, C. Pellicchia, *Macromolecules*, 2009, **42**, 5572. (m) G. Li, M. Lamberti, S. D'Amora, C. Pellicchia, *Macromolecules*, 2010, **43**, 8887. (n) J.-W. Hsu, Y.-C. Lin, C.-S. Hsiao, A. Datta, C.-H. Lin, J.-H. Huang, J.-C. Tsaic, W.-C. Hsueh, *Dalton Trans.*, 2012, **41**, 7700.
- 8 (a) A. C. Pinheiro, E. Kirillov, T. Roisnel, J.-F. Carpentier, O. L. Casagrande Jr, *Dalton Trans.*, 2015, **44**, 16073. (b) A. C. Pinheiro, A. H. Virgili, T. Roisnel, E. Kirillov, J.-F. Carpentier, O. L. Casagrande Jr, *RSC Adv.*, 2015, **5**, 91524.
- 9 (a) X. Ji, W. Yao, X. Luo, W. Gao, Y. Mu, *New J. Chem.*, 2016, **40**, 2071. (b) E. Kirillov, T. Roisnel, J.-F. Carpentier, *Organometallics*, 2012, **31**, 3228. (c) K.-T. Wang, Y.-X. Wang, B. Wang, Y.-G. Li, Y.-S. Li, *Dalton Trans.*, 2016, **45**, 10308. (d) J.-W. Hsu, Y.-C. Lin, C.-S. Hsiao, A. Datta, C.-H. Lin, J.-H. Huang, J.-C. Tsaic, W.-C. Hsueh, *Dalton Trans.*, 2012, **41**, 7700.
- 10 (a) L. Falivene, R. Credendino, A. Poater, A. Petta, L. Serra, R. Oliva, V. Scarano, L. Cavallo, *Organometallics*, 2016, **35**, 2286. (b) SambVca 2.0: a web application for analyzing catalytic pockets <https://www.molnac.unisa.it/OMtools/sambvca2.0/>.
- 11 All attempts to determine the viscosity-average molecular weight of the PE using the standard method (modified Ubbelohde viscometer, decaline at 135 °C using concentrations of 0.1 g dL<sup>-1</sup>) failed due to the partial solubilization of the polymers and/or formation of gel. Solubility of the PEs could be achieved only at 165 °C but all solutions returned precipitates while transferred to the viscometer operating at 135 °C.
- 12 F. S. Gomes, A.L. Bergamo, O. L. Casagrande Jr., *Macromol. Chem. Phys.*, 2014, **215**, 1735.
- 13 (a) S. Murtuza, O.L. Casagrande Jr., R.F. Jordan, *Organometallics*, 2002, **21**, 1882. (b) M. Bochmann, S. J. Lancaster, *Angew. Chem., Int. Ed. Engl.*, 1994, **33**, 1634. (c) I. Kim, R. F. Jordan, *Macromolecules*, 1996, **29**, 489. (d) I.

---

Tritto, R. Donetti, M. C. Sacchi, P. Locatelli, G. Zannoni,  
*Macromolecules*, 1997, **30**, 1247.